To appear in *Structure and Infrastructure Engineering*
Vol. 00, No. 00, Month 20XX, 1–18

Original Paper

Dynamic characterization of wind turbine towers account for a monopile foundation and different soil conditions

Pedro Galvín*, Antonio Romero, Mario Solís, José Domínguez

Escuela Técnica Superior de Ingeniería, Universidad de Sevilla, Camino de los Descubrimientos, 41092 Sevilla, Spain

()

The response of wind turbines is induced by dynamic loads such as wind, transient and cyclic loads, and also extreme loads such as earthquakes. Thus, the structural design requires an accurate evaluation of the modal parameters of the system because it is strongly required that no resonances are excited. Moreover, it has been concluded from previous research works that soil-structure interaction (SSI) should be accounted for the analysis. In the present paper, the structural dynamic response of wind turbine towers is investigated considering different soil conditions using a numerical model. This research is focused on SSI effects. Firstly, changes in the modal parameters of three different wind turbines considering the effect of three soils are evaluated. The results show that the evaluation of the natural frequency and the resulting classification of the wind turbine design type can be affected by SSI. The obtained results could be used to evaluate the decrement of the natural frequency of the wind turbine account for the soil and the foundation in relation to the frequency computed without soil interaction. Next, the seismic response of the wind tower is analysed considering two seismic events: a horizontally polarized shear (SH) incident wave and El Centro earthquake.

Keywords: soil-structure interaction; wind turbine; dynamic analysis; natural frequencies; foundation stiffness; seismic analysis; structural models; design

1. Introduction

European Wind Energy Association (EWEA) expects 192 GW of wind installations to produce 442 TWh meeting 14.9% of electricity consumption in 2020. This scenario will result in cumulative installations of 75 GW and an investment volume in wind farms of between €90 billion and €124 billion. By 2020, 354000 people will be employed in the European wind industry (EWEA (2014)). Nowadays, there are 117 GW wind power installations in the European Union and it is expected the installations expand to 192 GW in 2020 by the construction of 58 GW onshore installations and 17 GW offshore installations (EWEA (2014)).

According to the previous data, the majority of wind turbines will continue being located onshore due to lower construction costs. However, the new installations are a challenge for civil engineering: slender turbines with tower heights of more than 100 m are being built. The wind turbine dynamic responses are characterized from their natural frequencies, mode shapes and modal dampings.

The dynamic response of the wind turbines is due to loads from the wind turbulence, transient loads from operational procedures, and cyclic loads from the rotor frequency generated by mass imbalance in the blades and the frequency due to shadowing effects from the wind each time a blade passes the tower (Damgaard et al. (2014); IEC (2005); Lombardi et al. (2013)). The operational speed of the rotor of state-of-the-art wind turbines is typically about $5 - 15$ rpm. Three designs have been proposed to avoid the resonance of the system (Fischer (2006); Kühn (2003)):

*Corresponding author. Email addresses: pedrogalvin@us.es, aro@us.es, msolis@us.es, jose@us.es

- Soft-soft design, where the resonance frequency of the structure is lower than the rotor frequency (1 P).
- Soft-stiff design, where the resonance frequency is in the range between the rotor frequency (1 P) and the blade passing frequency (1 P times number of blades).
- Stiff-stiff design, where the resonance frequency is higher than the blade passing frequency.

The design procedure requires an accurate evaluation of the natural frequency of the system which involves the structure, the foundation and the surrounding soil. The soft-stiff is the most common design since fatigue can occur in the soft-soft design, and the cost associated with a stiff foundation makes the stiff-stiff design wasteful (Damgaard et al. (2014)).

The dynamic behaviour of wind turbines can be studied using numerical models and experimental procedures. Adhikari and Bhattacharya (2011, 2012) developed an analytical model based on an Euler-Bernoulli beam-column with elastic end supports. The elastic end-supports were considered to model the flexible nature of the interaction of these systems with soil. The proposed model was experimentally validated by a scale model of a Vestas V90 3 MW wind turbine with a monopile type foundation. Bhattacharya and Adhikari (2011) also modelled the foundation by two springs (translational and rotational). They concluded that the frequency of vibration is strongly related to the stiffness of the foundation, and generally the analytical model overestimated the natural frequency. They deeply studied a monopile foundation but the approach can be also used for suction caisson, multipod and concrete raft foundations. The translational and the rotational spring constants can be obtained from experimental methods. Andersen et al. (2012) presented a comprehensive study on the stiffness of a monopile foundation supporting an offshore wind turbine having a spatial variation of the soil properties by a simple model. Damgaard et al. (2013) presented the experimental investigation performed on offshore wind turbines supported by a monopile foundation for different wind parks in the period 2006-2011. They evaluated the first natural frequency and modal damping of the structures. Zania (2013) presented an analytical model to obtain the natural frequency and damping of the wind turbine system which accounts for the soil-pile interaction. In the cited work, the author also carried out a parametric study to illustrate the sensitivity of the resonance frequency on two dimensionless parameters (slenderness ratio and relative soilpile stiffness), as well as the pile's diameter and the pile tip boundary conditions (pinned and clamped). From this study, Zania concluded that the dynamic soil-structure interaction may lead to an advantageous design to restrictive frequency ranges. Damgaard et al. (2014) presented an efficient approach to evaluate the aeroelastic response with focus on monopile foundations. They showed that the effect of soil-structure interaction is critical for the design. In addition, they concluded that simplified foundation modelling approaches are only able to capture the dynamic response reasonably well after tuning of the first natural frequency and damping. Harte et al. (2012) studied the dynamic interaction effects between an embedded rigid gravity based foundation and the underlying soil, as softer soils can influence the dynamic response of wind turbines using an Euler-Lagrangian approach. This model showed that the dynamic response was significantly affected due to the soil-structure interaction. Lombardi et al. (2013) carried out a series of laboratory tests in which a scaled model wind turbine supported on a monopile in kaolin clay was subjected to dynamic loading. The measured natural frequency was found to be strongly dependent on the shear strain level in the soil next to the pile. They proposed a practical guidance for choosing the diameter of monopile. Bhattacharya et al. (2013) developed a small scaled tests of wind turbine model on three types of foundations: monopiles, symmetric tetrapod and asymmetric tripod. They concluded that the number of cycles to failure may increase for symmetric foundations. Shirzadeh et al. (2013) identified the natural frequency and the damping from ambient response, and they proposed a numerical model taking into account the soil-pile interaction. Simulation results were in good agreement with the measurement data.

In relation to the dynamic response, Hermanns et al. (2011) studied the dynamic response of a wind turbine structure subjected to theoretical seismic motions taking into account the rotational component of ground shaking. Von Mises stress values at different heights of the tower were used

to study the dynamical structural response to a set of synthetic ground motion time histories. The results obtained in this study indicated the importance of the rotational components of ground motions on wind turbine response patterns. Van der Woude and Narasimhan (2014) discussed the use of vibration isolation to reduce the dynamic response of wind turbine structures, with emphasis on the structural response to seismic loading. In the two previous studies, soil-structure interaction was not considered. Kjørlaug et al. (2014) presented a study of the seismic response of wind turbines. In that case, the surrounding soil was included in the model in order to account for the soil-monopile-structure interaction. The obtained results showed that earthquake was not expected to govern the design for small to moderate earthquakes in stiff soils. However, for softer soils, the displacement and base moment demand from the earthquake could very well match the response from wind-induced forces. Sapountzakis et al. (2015) accounted for the soil-structure interaction and the non-linear behaviour in the dynamic analysis of a wind turbine tower founded on monopile foundation system. The results of the proposed model illustrated the strong influence of the non-linear effects on the dynamic response of the wind turbine tower. Negro et al. (2014) summarized uncertainties for offshore wind foundations design, and they exposed doubts and solutions. Bisoi and Haldar (2014) presented a comprehensive study on the dynamic behaviour of offshore wind turbine structure supported on monopile foundation in clay by the finite element method. This study showed that tower deflection, rotation and bending moment increased with foundation flexibility; the monopile head rotation and deflection increased with the cyclic $p-y$ curve; the response of the system increased with soil stiffness degradation effect; monopile response decreased significantly due to an increase in soil stiffness; tower and monopile responses under extreme wind event substantially increased with the incorporation of soil non-linearity; the responses of monopile and tower decreased initially with the embedded length; and the maximum lateral deflection at tower top increased with tower height. Bisoi and Haldar (2015) investigated the feasibility of soft-soft and soft-stiff design approaches considering two monopile supported three bladed offshore wind turbines founded in clay.

From the previously mentioned researches and others (Clouteau et al. (2013); Kausel (2010); Wolf (1985)) it can be concluded that the dynamic response of a wind turbine structure depends on the properties of the soil where it has been built. The results indicated that, if a rigid base condition is considered, the natural frequencies of the structure on soft soil are significantly overestimated and the damping ratios are underestimated. Moreover, the foundation and the soil can greatly influence the overall wind turbine response. Therefore, soil-structure interaction (SSI) is important and cannot be neglected in this type of problems. The wind turbine design process needs an accurate evaluation of the modal parameters (natural frequencies, mode shapes and modal dampings) accounting for the tower, the foundation and the surrounding soil because the stability, operation and safety depend on them.

The aim of this research is to investigate the structural dynamic response of wind turbines considering different soil conditions using a fully coupled three-dimensional boundary element-finite element model. The presented results can be used to approach the natural frequencies of the system taking into account the soil properties, and to effectively determine the actual wind turbine design from the previous estimations and the rotor frequency (soft-soft, soft-stiff or stiff-stiff). The outline of the paper is as follows. In Section 2, the numerical model is presented including a brief summary of the finite element and the boundary element time domain formulations. Next, the influence of the soil on the response of the wind turbine is analysed. Several numerical studies are developed. Firstly, in Section 3, a modal analysis is done. The Frequency Response Functions (FRFs) are used for an accurate identification of natural frequencies. FRFs are computed as the relationship between an impulsive input force and the structural response in the frequency domain. The FRFs of the soil-pile system are obtained for horizontal and vertical impulse forces. These FRFs are used to compute the first natural frequency of the soil-pile system as well as its dynamic stiffness in both horizontal and vertical directions. The obtained results are used for verification of the methodology by comparison with previous researches, and also to show the influence of SSI effects. The FRF of the overall system is obtained from the response to a horizontal impulsive load applied at the

top of the tower. Only a horizontal load is considered since it provides a good approach of the structural dynamic response to operational loads. Secondly, in Section 4, the seismic response of the wind tower is analysed considering two events: a horizontally polarized shear (SH) incident wave and El Centro earthquake. A SH wave produces displacements perpendicular to the direction of wave propagation and it is totally reflected at the free surface. Therefore, this study provides information about the structural bending response due to any seismic load. The seismic response to the well-known El Centro earthquake, which seismic accelerogram has been extensively used in the literature, is also studied as a comprehensive case study. In this case, the waves produced displacements in all directions. Finally, based on all the obtained numerical results, conclusions are drawn in Section 5.

2. Numerical model

This research uses a numerical method based on a three dimensional (3D) boundary element-finite element (BEM-FEM) coupled formulation in time domain (Galvín and Romero (2014)). The proposed model allows to study soil-structure interaction (SSI) problems by domain decomposition in two subdomains represented by the BEM and FEM. The BEM formulation can efficiently solve wave propagation problems, since the radiation condition is implicitly satisfied in the fundamental solution. The radiation condition states that no energy may be radiated from infinity into the dynamic system for a load applied to the structure or for the scattered motion in the case of e.g. seismic load (Eringen and Suhubi (1975)). For that reason, FEM formulation requires the use of appropriate boundary conditions or fictitious absorbing medium to attenuate the spurious reflections at the mesh boundaries. Therefore, in the present research, the soil behaviour was represented by the BEM, whereas the structures (foundation and tower) were modelled with the FEM, since it is advantageous for modelling complex geometries and non-linear behaviour. For the BEM, this work used the full-space Green's functions, considering the internal soil damping directly in the time domain formulation (Galvín and Domínguez (2007)).

The BEM is based on a time marching procedure to obtain the time variation of the boundary unknowns; i.e. displacements and tractions. The k component for displacements and tractions over the boundary are approximated from their nodal values j at each time step m, u_k^{mj} and p_k^{mj}, using the space interpolation functions $\phi^j(r)$ and $\psi^j(r)$. After interpolating the boundary variables, the integral representation of the displacement u at a point i on the boundary becomes (Romero et al. (2013)):

$$c_{lk}^i u_k^i(\mathbf{x}^i,t) = \sum_{m=1}^{n}\sum_{j=1}^{Q}\left\{\left[\int_{\Gamma_j} U_{lk}^{nm}\psi^j\, d\Gamma\right] p_k^{mj} - \left[\int_{\Gamma_j} P_{lk}^{nm} d\tau\phi^j\, d\Gamma\right] u_k^{mj}\right\} \tag{1}$$

where Q is the total number of boundary nodes and Γ_j represents the elements to which node j belongs. Time kernels U_{lk}^{nm} and P_{lk}^{nm} are respectively computed through the fundamental solution for displacements and tractions due to a point load at $\mathbf{x}^i$ acting in l direction. These kernels are analytically integrated using constant and linear piecewise time interpolation functions for tractions and displacements (Galvín and Domínguez (2007)), respectively. Equation (1) is written in a more compact form as:

$$c_{lk}^i u_k^{ni} = \sum_{m=1}^{n}\sum_{j=1}^{Q}\left[G_{lk}^{nmij} p_k^{mj} - \widehat{H}_{lk}^{nmij} u_k^{mj}\right] \tag{2}$$

Once the integral-free term c_{lk}^i is included in the system matrix, the integral representation for

point i at time $t = n\Delta t$ becomes:

$$\mathbf{H}^{nn}\mathbf{u}^n = \mathbf{G}^{nn}\mathbf{p}^n + \sum_{m=1}^{n-1}[\mathbf{G}^{nm}\mathbf{p}^m - \mathbf{H}^{nm}\mathbf{u}^m] \tag{3}$$

where H_{lk}^{nmij} collects for c_{lk}^{i} when $i = j$ and $n = m$.

The FEM equation at each time step n is defined as Zienkiewicz (1986):

$$\mathbf{M}\ddot{\mathbf{u}}^n + \mathbf{C}\dot{\mathbf{u}}^n + \mathbf{K}\mathbf{u}^n = \mathbf{f}^n \tag{4}$$

where $\mathbf{M}$, $\mathbf{C}$ y $\mathbf{K}$ are mass, damping, and stiffness matrices, respectively. $\mathbf{u}^n$, $\dot{\mathbf{u}}^n$ and $\ddot{\mathbf{u}}^n$ represent nodal displacement, velocity, and acceleration, respectively, and $\mathbf{f}^n$ is the load vector.

Equation (4) is solved using an implicit time integration GN22 Newmark method (Newmark (1959); Zienkiewicz (1986)). An equivalent dynamic stiffness matrix $\mathbf{D}$ is defined as:

$$\mathbf{D}\mathbf{u}^n = \mathbf{f}^n + \mathbf{f}^{n-1} \tag{5}$$

Coupling of BEM and FEM (Equations 3 and 5) is carried out by imposing equilibrium and compatibility conditions at the soil-structure interface. Both systems of equations are assembled into a single global system, together with the equilibrium and compatibility equations (Prabucki and von Estorff (1990)).

This work used the `SSIFiBo` toolbox for `MATLAB` previously developed by Galvín and Romero (2014); Romero et al. (2013) and Galvín et al. (2010). The FEM module of the toolbox does not include any pre-processor. Instead, a gateway for commercial software allows importing directly the structure model.

3. Response of wind turbines on monopiles

This study includes the interaction between the foundation and the underlying soil, and the dynamic behaviour of the coupled system wind turbine structure-foundation-soil.

Three 3 MW wind turbines were analysed in this research: model 1, model 2 and model 3. Each turbine model corresponds to a different design approach (soft-soft, soft-stiff and stiff-stiff). The rotor speed was $P = 0.25\,\text{Hz}$ (15 rpm) and the blade passing frequency was $3P = 0.75\,\text{Hz}$. Let h stand for the tower height measured from the pile cap (Figure 1.(a)). A mass $m = 112.1 \times 10^3\,\text{kg}$ at the top of the tower represents the blades, the nacelle and the hub nose cone. The tower is modelled by an equivalent mass per unit length $\rho_t A_t$ and an equivalent bending stiffness $E_t I_t$, since only its global modal parameters are of interest for this study. Therefore, the variability of the tower's cross section was not considered. Table 1 shows the equivalent geometrical properties of the three models of turbines. They correspond to the different design approaches depending on h, A_t and I_t parameters.

The steel tower material properties were: Young's modulus $E_t = 210 \times 10^9\,\text{N/m}^2$, Poisson's ratio $\nu_t = 0.3$, and density $\rho_t = 7850\,\text{kg/m}^3$. A bilinear kinematic hardening material model was considered with the following properties: yield stress $\sigma_t^y = 275 \times 10^6\,\text{N/m}^2$ and tangent modulus $E_t^t = 136 \times 10^9\,\text{N/m}^2$. Structural damping ratio was estimated at 2% for all modes that contribute significantly to the structure response. The damping matrix was computed proportionally to the mass and the stiffness matrices (Clough and Penzien (1975)) ($\mathbf{C} = \alpha_0\mathbf{M} + \alpha_1\mathbf{K}$). Table 1 also presents the design approach of the wind turbines, obtained by comparison of P and the first natural

frequency of the wind-turbine neglecting the soil-foundation-structure interaction. The expression given by Tempel and Molenaar (2002) was used: $f_1 \approx \sqrt{3.04 E_t I_t/((m + 0.227\rho_t A_t h)4\pi^2 h^3)}$. The structure was founded with a single concrete pile of $d = 2.2\,\mathrm{m}$ diameter and $L = 50\,\mathrm{m}$ depth, with Young's modulus $E_p = 30 \times 10^9\,\mathrm{N/m^2}$, Poisson's ratio $\nu_p = 0.25$, and density $\rho_p = 2500\,\mathrm{kg/m^3}$. The geometrical properties of the concrete monopile were obtained from the research presented by Bhattacharya and Adhikari (2011) for a Vestas V90 wind turbine.

The structure rested on an elastic soil. The soil characteristics are shown in Table 2, where C_s, C_p and ρ_s are shear and dilatational wave velocities and soil density, respectively. Soil type F includes peat, highly organic clay, loose saturated sand or marshland; type E reproduces soft or silty clays; soil type D considers loose to very dense sands, silt loams, sandy clays, or medium stiff to hard clays; and type C includes soft rock, sandstones or gravels. The site classes and their shear wave propagation velocities are consistent with those presented in ASCE (2010). The soils are classified based on the upper 30 m of the site profile (Borcherdt (1994)). $C_p = 2C_s$ was considered, entailing a Poisson's ratio $\nu = 1/3$. The soil density was set equal to $1800\,\mathrm{kg/m^3}$ for all types of soils.

Table 1.: Turbine geometrical properties.

	h [m]	A_t [m^2]	I_t [m^4]	f_1 [Hz](without SSI effects (Tempel and Molenaar (2002)))	Design approach without SSI effects
Model 1	105	0.74	0.94	0.23	soft-soft
Model 2	105	1.16	3.52	0.39	soft-stiff
Model 3	70	1.16	3.52	0.81	stiff-stiff

Table 2.: Soil characteristics.

	C_s [m/s]	C_p [m/s]	ρ_s [kg/m^3]
Type C	365	730	1800
Type D	250	500	1800
Type E	150	300	1800
Type F	80	160	1800

Figure 1.(b) shows the problem discretization. The structure was modelled with 105 two-node Euler-Bernoulli beam finite elements and a one-node mass finite element on top of the structure, while the pile was represented with 2400 eight-node solid finite elements. The pile cap was modelled with 48 rigid four-node shell elements. The soil was represented by 332 quadratic nine-node boundary elements. A circular area with a radius of 10 m around the tower was considered to be enough for modelling the soil surface (Domínguez (1993)). The nodes of the boundary and finite elements at the pile-soil interface had the same degrees of freedom (displacements at the three spatial directions). Therefore, a conventional technique for coupling matching meshes was employed. The same soil-foundation discretization was used for the different numerical simulations. The time step Δt was chosen to compute results in the frequency range of interest, i. e., the frequencies where the modal parameters of the system were expected according to the previous expression (Tempel and Molenaar (2002)), but also accounted for the stability requirements of the BE time domain formulation (Galvín and Domínguez (2007)). A maximum frequency of 15 Hz was studied. The minimum value of the stability parameter $\beta = C_s \Delta t/l$, where l is the distance between two adjacent nodes of a boundary element, was set equal to 0.6. The resulting time steps were 0.0034 s, 0.0050 s, 0.0083 s and 0.0156 s for soil types C, D, E and F, respectively.

3.1. *Dynamic soil-pile stiffness*

The dynamic behaviour of a wind turbine is strongly affected by the soil-pile response. Therefore, the identification of the natural frequencies of the soil-pile system is an important point to distinguish between the local soil-pile effects and the overall structural responses. Moreover, displacements at the pile cap could affect the operational conditions of the structure. In this section,

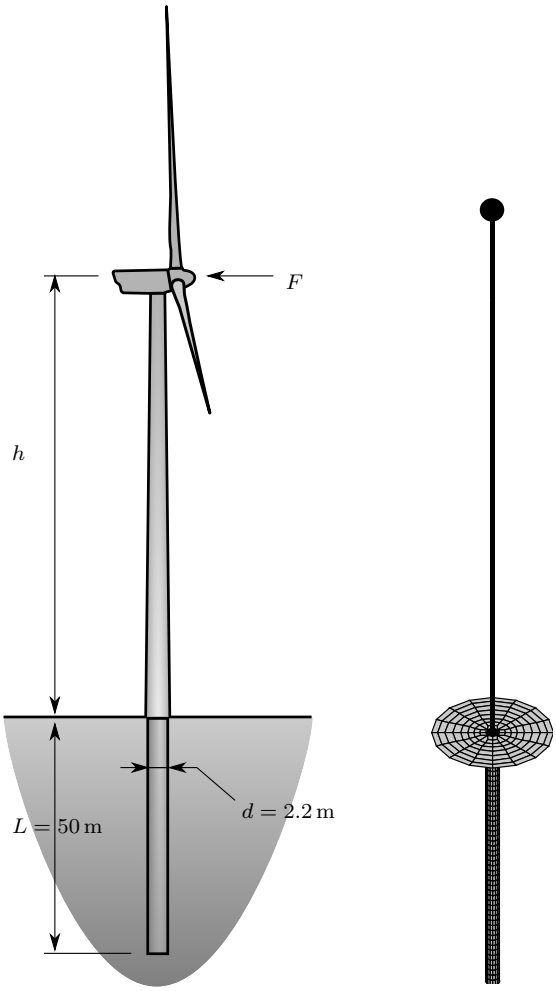

Figure 1.: (a) Wind-turbine geometry and (b) BEM-FEM model.

the horizontal (k^s_{xx}) and vertical (k^s_{zz}) dynamic soil-pile stiffnesses are computed. The present analysis is about the foundation behaviour, and it only includes the pile and soil discretization.

An impulsive load $p^\delta(t) = p_0\delta(t)$ (being $p_0 = 1\,\text{N}$ and $\delta(t)$ the Dirac delta function), was applied at the center of the pile-cap to compute its frequency response function. Horizontal and vertical forces were studied. The soil-pile dynamic stiffness was computed from pile-cap displacements. Figure 2 presents the comparison between the computed results and the reported ones by Kaynia and Kausel (1991) to show the capabilities of the proposed methodology. The proposed model accounted for translational and rotational components of the ground motion of the pile cap. However, the rotational stiffness was omitted in Kaynia and Kausel (1991) and it is not presented here. The stiffness components were normalized by the corresponding static pile stiffness (Table 3) and they were represented versus the dimensionless excitation frequency $a_0 = \omega d/C_s$, where ω was the angular frequency and d was the pile diameter.

The work presented by Kaynia and Kausel (1991) was used for comparison purpose since the properties they used almost match with those studied in Bhattacharya and Adhikari (2011). The results presented in Kaynia and Kausel (1991) were obtained for soil type D. However, Kaynia and Kausel (1991) analysed a pile with a relation $L/d = 20.0$, while Bhattacharya and Adhikari (2011) and the present manuscript consider a relation $L/d = 22.7$. The proposed BEM-FEM model slightly underestimated the stiffness at lower frequencies and overestimated it at higher frequencies. Figure 3 shows the relative error between both results. The largest percent difference in horizontal normalized stiffness was 13.3% and 8.1% in the vertical direction at $a_0 = 1$. The discrepancies

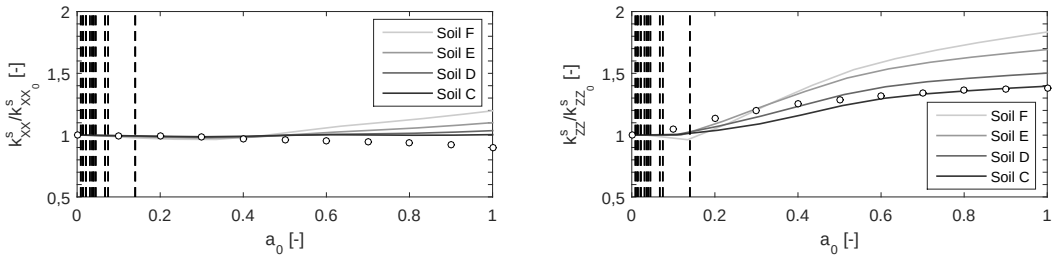

(a) (b)

Figure 2.: (a) Horizontal and (b) vertical soil-pile normalized stiffness considering soil types C, D, E and F (dark grey to light grey lines) and Kaynia and Kausel (1991) model (circles). Vertical dashed black lines indicate the first natural normalized frequencies for the wind turbines without SSI

.

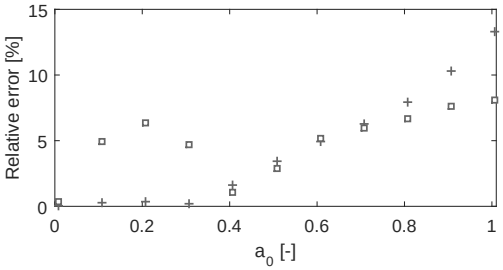

Figure 3.: Relative difference between the results computed from the proposed model and those presented by Kaynia and Kausel (1991): horizontal (crosses) and vertical (squares) soil-pile normalized stiffness considering soil type D.

between both set of results was significant. They could be partly due to the approximations of every methodology and the different properties. Nevertheless, at the frequency range below $a_0 = 0.2$, where the first natural frequencies of the system was expected from the expression given by Tempel and Molenaar (2002) and that it is shown in the Figure 2, the maximum relative error was lower than 5.0%.

Figure 4 shows the imaginary part of the horizontal and vertical Frequency Response Function (FRF) of the soil-pile system considering the different soils. The resonance frequencies of the soil-pile system were obtained from the peaks appearing in those functions. It can be appreciated that the resonance frequency for the lateral displacement occurred at the same normalized frequency $a_0 = 2.8$. However, no clear patterns appeared at the vertical direction.

Table 3 also shows the horizontal and vertical natural frequencies of the pile-soil systems. These values can be used to obtain the effective length of the pile for dynamic loading using the classical expression for the first resonant frequency of a closed pipe: $f = c_p/4L = \sqrt{(E_p/\rho_p)}/4L$, where L is the effective length of the pile. The obtained active lengths of the pile were 12 m, 17 m, 28 m and 50 m for the soils C, D, E and F, respectively.

Table 3.: Static soil-pile stiffness ($a_0 = 0$) and natural frequencies.

	Soil type C	Soil type D	Soil type E	Soil type F
$k^s_{xx_0} \times 10^9$ [N/m]	2.38	1.24	0.52	0.18
$k^s_{zz_0} \times 10^9$ [N/m]	7.13	4.74	2.54	0.98
$f_{\text{horizontal}}$ [Hz]	72	49	30	16
f_{vertical} [Hz]	105	60	34	23

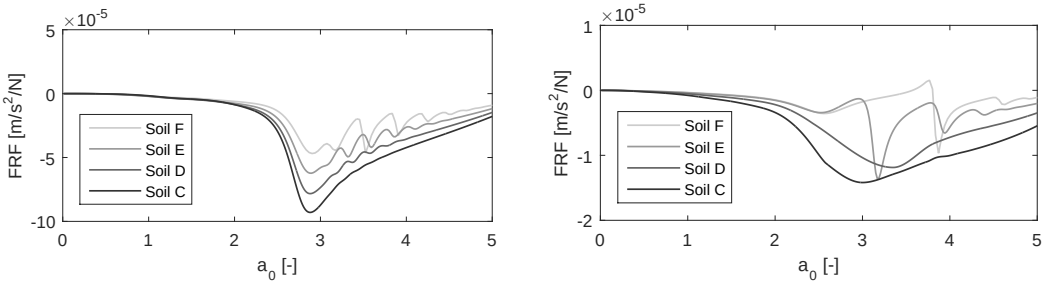

Figure 4.: Imaginary part of the (a) horizontal and (b) vertical frequency response function of the soil-pile system considering soil types C, D, E and F (dark grey to light grey lines).

3.2. *Dynamic response considering soil-structure interaction*

In this section, soil-structure interaction effect was assessed through nacelle dynamic response due to an impulsive load applied atop the wind turbine. The full-coupling model presented in Figure 1.(b) was considered. The time history of the horizontal displacement was computed using the numerical methodology. Then, the frequency response was obtained by applying a direct Fourier Transform to the time response.

Table 4.: Wind turbine natural frequencies f [Hz] and damping ratio of first mode shape ξ [-].

		without soil	Soil type C	Soil type D	Soil type E	Soil type F
Model 1	f_1	0.23	0.16	0.16	0.16	0.14
	f_2	1.56	1.22	1.20	1.18	1.12
	f_3	4.48	3.78	3.72	3.64	3.50
	ξ	0.0296	0.0451	0.0610	0.0624	0.0650
Model 2	f_1	0.39	0.18	0.16	0.16	0.14
	f_2	2.50	1.80	1.78	1.74	1.66
	f_3	7.02	5.52	5.44	5.40	5.26
	ξ	0.0305	0.0421	0.0494	0.0507	0.0597
Model 3	f_1	0.81	0.30	0.28	0.26	0.24
	f_2	5.32	3.74	3.66	3.50	3.22
	f_3	14.50	11.96	11.92	11.68	8.34
	ξ	0.0197	0.0237	0.0286	0.0278	0.0315

Figure 5 shows the FRFs from 0 Hz to 2 Hz of the three turbine models when a horizontal impulsive load F (Figure 1.(a)) was applied. The time history of the applied load was a Dirac delta function. The first three bending natural frequencies of the tower and the damping ratio of the first mode shape are presented in Table 4. It should be mentioned that only the tower and the mass of the blades, the nacelle and the hub nose cone were considered in the case without soil. In this case, neglecting the SSI, the first natural frequencies computed for the three turbine models agreed with those obtained from the expression gave by Tempel and Molenaar (2002) (Table 1).

When SSI is considered, the damping of the soil-pile system affects the damping of the overall system and its natural frequencies decreases when the soil is softer. For example, the first natural frequency of the turbine model 3 for the softest soil moved from 0.81 Hz when the SSI was not considered to 0.24 Hz when it was.

Shirzadeh et al. (2013) presented an experimental research about the dynamic behaviour of a Vestas V90 3 MW offshore wind turbine 72 m above sea level founded by a monopile on a stiff soil. The operational interval of the turbine was $8.6 - 18.4$ rpm. The measured response of the structure was mainly controlled by its first natural frequency at 0.35 Hz. Therefore, taken into account the importance of the first natural frequency for the entire system, Figure 6.(a) shows its decrement for the three wind turbine models accounting for the SSI in relation to the frequency computed without SSI. The highest decrement appeared for the model 3 (that corresponds to a stiff-stiff

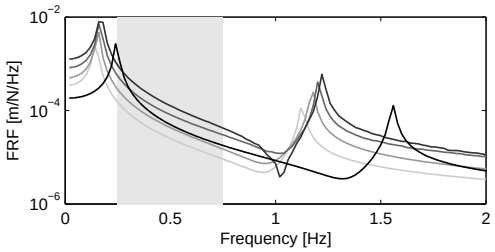

(a)

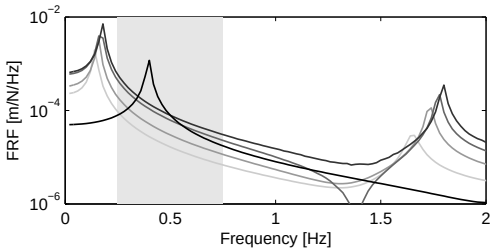

(b)

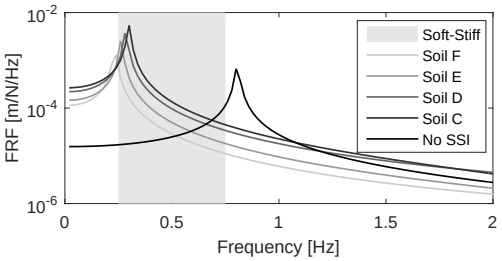

(c)

Figure 5.: Frequency content of the FRF of wind turbines (a) model 1, (b) model 2 and (c) model 3 due to a horizontal impulsive load without soil-structure interaction and considering soil types C, D, E and F (black to ligth grey lines). The soft-stiff design is limited by the grey area.

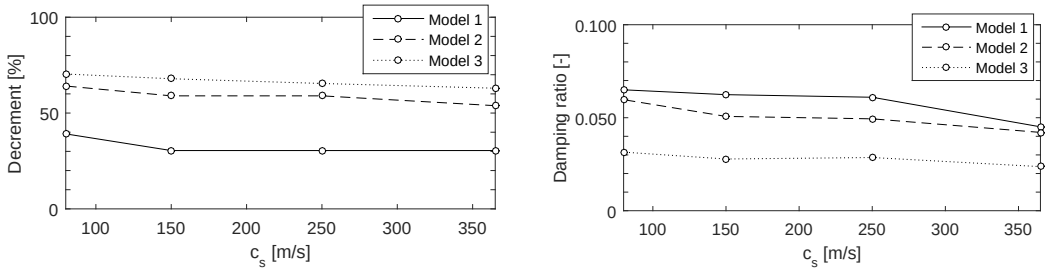

(a) (b)

Figure 6.: (a) Decrement of the first natural frequency and (b) damping ratio of the first mode shape for the wind turbine model 1 (black solid line), model 2 (dashed line) and model 3 (dotted line) considering the four different soils.

design when SSI is not considered). It exhibited a decrement of about 60% that was practically not dependent on the soil. These results show that SSI effects should be considered in wind turbine design when a particularly careful analysis is required to ensure that no resonances are excited (Manwell et al. (2002)).

The frequency shift showed in Figure 5 illustrates that SSI effects should be considered in order to

avoid dynamic effects related with the excitation of resonance frequencies in operation conditions. Moreover, the design approach (Table 1) based on the values of the natural frequencies obtained without considering SSI effects also changed: turbine models 1 and 2 turned to be soft-soft, and turbine model 3 was stiff-soft except for the softest soil. It should be mentioned that the soft-soft design is generally less expensive because it is lighter, but it could be affected by fatigue due to cyclic loads (Damgaard et al. (2014); Manwell et al. (2002)). Thus, the change to an actual soft-soft design is not on the side of safety. The natural frequencies computed by the proposed model were lower than the values obtained from Tempel and Molenaar (2002), since the soil-foundation system was not considered in their formulation. Nevertheless, several authors have proposed more comprehensive analytical models for estimating the natural frequencies of wind turbines accounting for the soil-foundation system (Adhikari and Bhattacharya (2011, 2012); Bhattacharya and Adhikari (2011); Harte et al. (2012); Zania (2013)).

Figure 7 shows the estimated mode shapes considering soil type F and without SSI. The mode shapes are presented to illustrate changes on the deformed shape of the tower at operational conditions. It can be observed that the first bending mode shapes were slightly modified by the effect of SSI. However, the second (dark grey line) and the third (black line) mode shapes were significantly affected. For both mode shapes, the points where the modal amplitude is zero, shifted to a lower height, and modal curvatures along the tower were smoother when the soil was accounted for in the analysis. Moreover, the shape of mode 3 is significantly modified by the effect of SSI for turbine models 2 and 3. When the soil and the foundation were not considered, displacements were fixed at the pile cap. This boundary condition was relaxed when the pile was taken into account. Then, pile cap displacements occurred according to the response function at the corresponding frequency (Figure 2). This phenomenon should be considered for the design.

Regarding damping ratios (Table 4) it can be observed that they increased as the soil was softer. This effect could be advantageous on design stages, and it must be mentioned that damping ratios are normally underestimated by simplified models because the damping due to the soil is neglected. In this paper, the damping ratios were estimated analysing the decay of the free vibration of the tower after the pulse loading. It was assumed that the decay had only the contribution of the first mode. This assumption can be accepted when damping is small and proportional and the modes are well separated. As a preliminary study, the aerodynamic damping was not considered. Alternatively, the damping ratio can be also determined by the half-power bandwidth method or more advanced methods (Magalhaẽs et al. (2010); Papagiannopoulos and Beskos (2006)).

4. Seismic Response

Finally, a case study concerning the seismic response of the wind turbines is considered. It was studied to illustrate the structural bending response due to an incident wave-field in the soil. For that purpose, two different wave-fields were considered: a SH incident wave and El Centro earthquake. The considered SH wave was a unit amplitude with an impulsive time variation. This incident wave-field produces vibrations perpendicular to the direction of wave propagation and it is totally reflected at the free surface. Therefore, the computed results provide useful information for analysing the structural horizontal response due to any incident wave-field such as an earthquake. The seismic response to El Centro earthquake, one of the major earthquakes that caused considerable damage, was also included as a case study. The seismic accelerogram of this earthquake is well-known and it has been extensively used in the literature. In this earthquake, the waves produced displacements in the horizontal and vertical directions. A single point response (SPR) excitation model, where the incident wave was transmitted simultaneously to all nodes of the pile, was use for both events.

Figure 8 shows the FRFs at the pile cap and at the nacelle due to horizontal impulsive SH incident wave-field with unitary amplitude. Firstly, some generalities are discussed. The structure

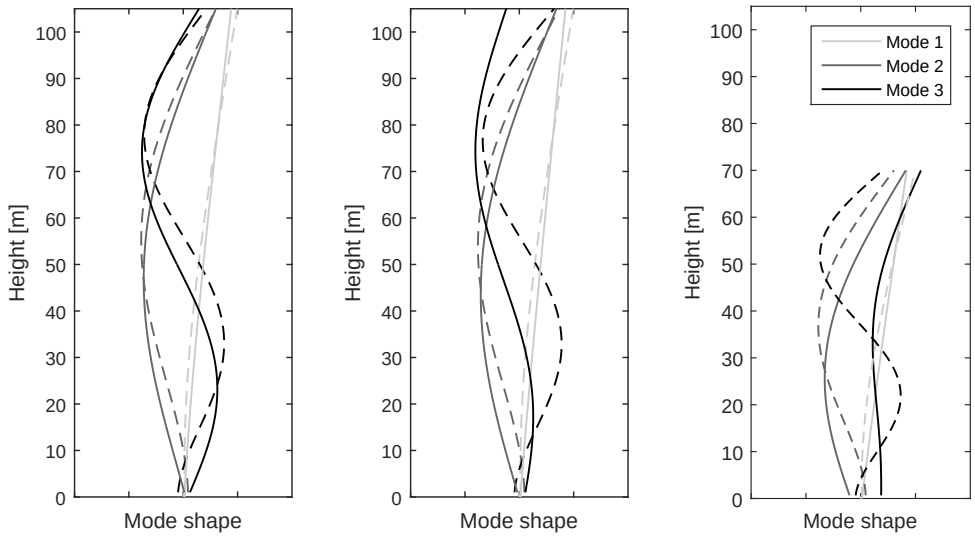

Figure 7.: Bending mode shapes of wind turbines (a) model 1, (b) model 2 and (c) model 3, without SSI (dashed line) and considering soil type F (solid line).

response tends to unitary amplitude at 0 Hz (static response) when excitation and response directions were coincident. The vertical responses due to the horizontal SH-wave were negligible and the corresponding figures have been omitted.

The response at the top of the foundation (Figures 8.(a,c,e)) remained constant for the case without SSI for all frequency range due to the high soil-foundation stiffness (equivalent to infinite). The constant value was equal to unity, as the value of the incident wave. In other cases, when SSI is considered, the horizontal responses (at the foundation as well as at the nacelle) showed amplifications around natural frequencies, which can be identified from the peaks on the frequency response of the structure. At the foundation, the response was dominated by the second natural frequency of the overall structure, which is higher than 1 Hz (Table 4). The response at the first natural frequency was attenuated by the damping of the soil-pile system. However, at the top of the wind tower, the effects of both frequencies were significant. The top tower accelerations (Figures 8.(b,d,f)) were approximately ten times higher than the foundation responses. The resonant peaks were clearly identified and they moved to lower frequencies when SSI was considered. Figure 8 shows that SSI effect induced a reduction of the response at natural frequencies due to a higher damping ratio. The damping can be estimated from these results by the half-power bandwidth method. The structural response induced by the impulsive SH wave in the frequency domain represents the FRF of the system. Therefore, the structural response due to any horizontal wave-field can be obtained from these results by superposition of the frequency content of the incident wave.

Next, the dynamic behaviour of the wind turbine due to El Centro (1940) seismic accelerogram was evaluated as a comprehensive case study. This historic earthquake is defined by energy distribution over a range frequency up to 5 Hz. Therefore, the stresses induced by the earthquake in the structure could be serious since the first and the second natural frequencies of the wind turbine were at this frequency range. The energy was concentrated mainly in the N-S component. The earthquake Arias Intensity was $I_A = 1.68\,\mathrm{m/s}$ (average of the two horizontal components). Figure 9 shows the time history, the frequency content and the pseudo-acceleration spectrum (PSA).

Figure 10 shows the response at the top of the pile and atop the tower for the wind turbine model 2 in the three orthogonal directions, according with the E-W, N-S and vertical components, considering the softest soil. This soil (type F) was selected for this case study since it was the more affected by seismic loads (Kjørlaug et al. (2014)). Moreover, the earthquake response can exceed the wind response for soft soils. Figure 10 shows that the maximum and minimum values in the

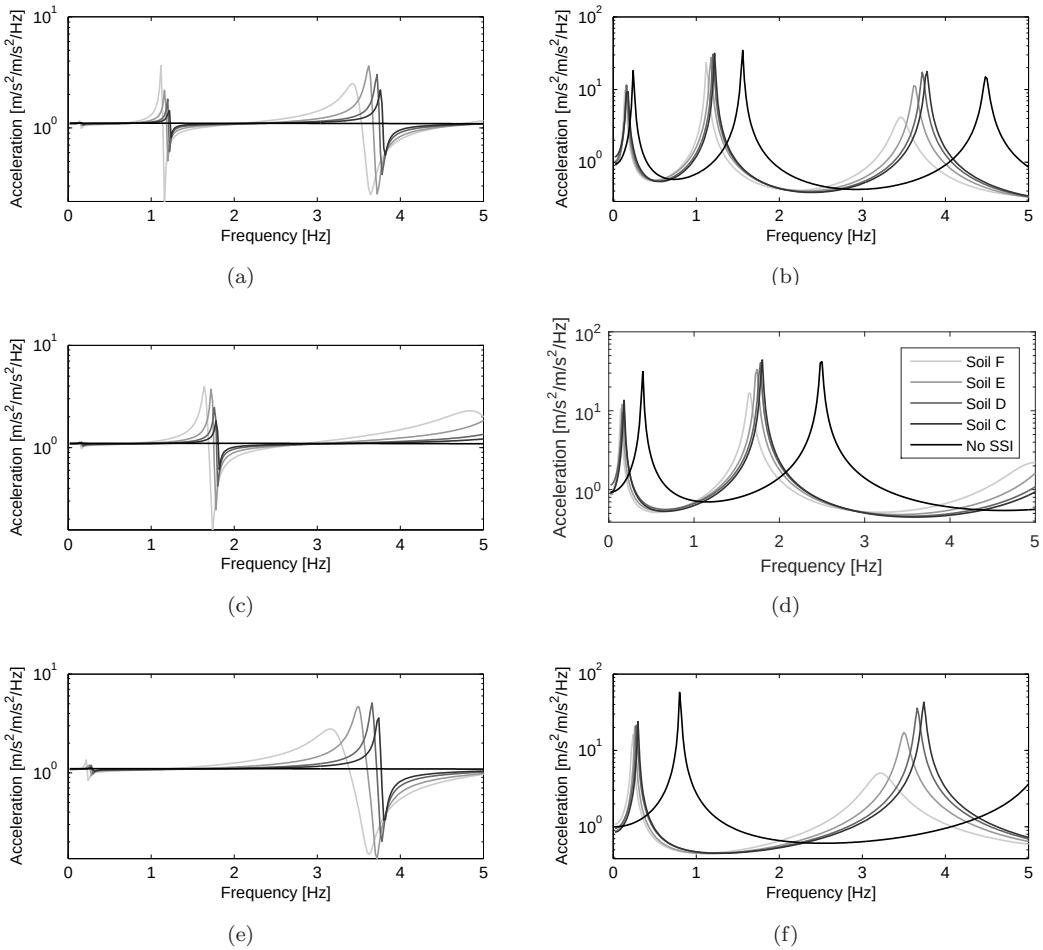

Figure 8.: Frequency content of the horizontal response (a,c,e) at the pile cap and (b,d,f) at the nacelle for wind turbine models (a,b) 1, (c,d) 2 and (e,f) 3 due to a horizontal impulsive SH wave without soil-structure interaction and considering soil types C, D, E and F (black to ligth grey lines).

time histories of the response occurred at the same time that in the seismic accelerogram. High amplifications can be observed atop the wind tower, with the maximum level in the N-S direction. The seismic wave field (Figure 9) was widely amplified in the response (Figure 10) about two times around 1.5 Hz.

The structural frequency responses show maximum levels around the second natural frequency at 1.66 Hz. This results agreed with the previous discussion and it can be explained from the FRF presented in Figure 8 and the earthquake PSA. The values of the PSA at the first natural frequency (0.14 Hz) were low and it was not expected that this mode contributed to the structural response although the FRF had a significantly amplitude at this frequency value.

Figure 10.(c) includes horizontal lines that presents the maximum absolute values of the acceleration computed from a seismic response spectrum analysis of the structure without SSI. The agreement between the maxima in the obtained time histories and the spectrum analysis was acceptable. However, structural behaviour was different: the response computed with the proposed model is dominated by the second bending mode shape, while, in the spectrum analysis, the response is mainly influenced by the first mode. This study illustrates the importance of the soil-structure interaction to predict the seismic response of wind turbines.

Finally, the stresses in the structure were computed and compared for three cases: (i) without SSI and linear analysis, (ii) considering SSI and linear analysis, and (iii) with SSI and non-linear

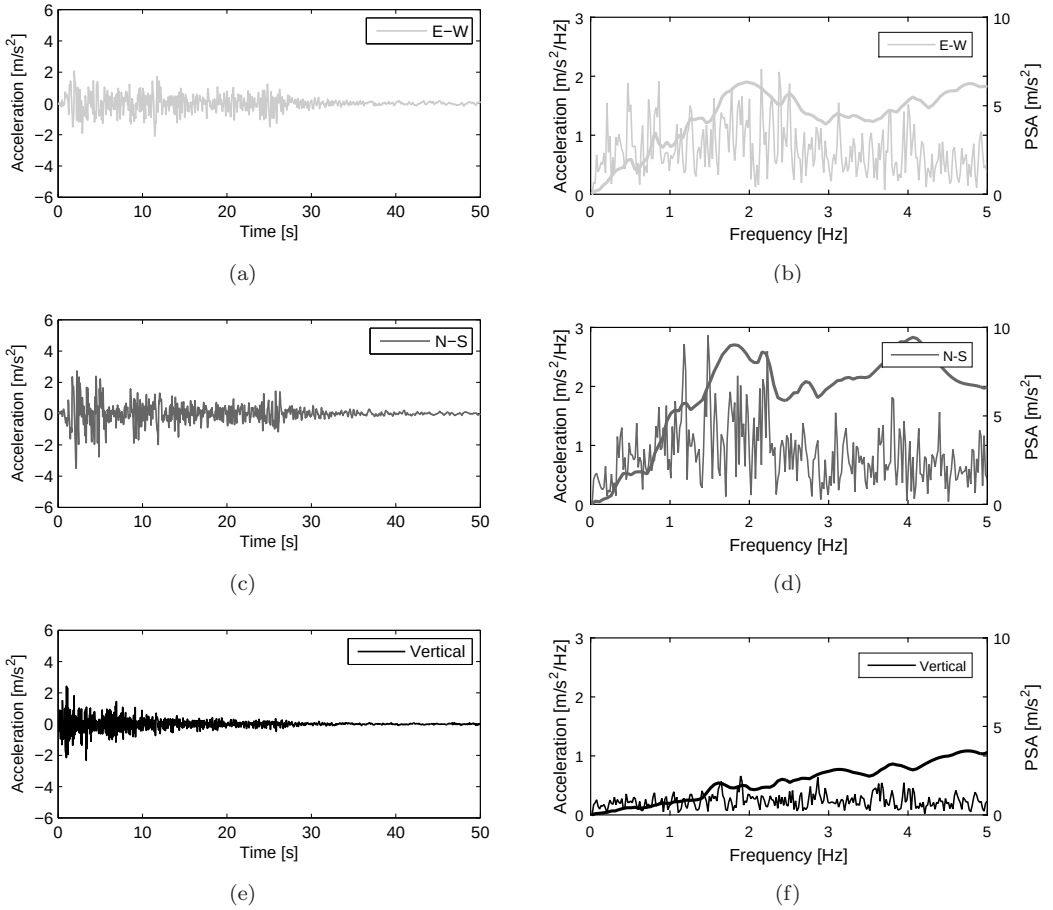

Figure 9.: (a,c,e) Time histories and (b,d,f) frequency content of acceleration and PSA (thick line) at E-W, N-S and vertical directions of El Centro (1940) accelerogram.

analysis. The linear and non-linear analysis refers to the consideration of an elastic or an bilinerar kinematic hardening constitutive law for the material of the tower, as defined in Section 3. The proposed methodology allowed to analyse all these situations that could also be of interest for addressing the structural response induced by wind or other loads. Figure 11 shows the time history of the equivalent stresses at the top of the foundation and at the half length of the tower. The stresses at the half length of the tower were studied because the highest values were expected there according to the deflection of the second mode. The equivalent stresses were normalized by the yield stress $\sigma_t^y = 275 \times 10^6\,\mathrm{N/m^2}$. The base moment demand increases as the soil was softer agree with the results presented by Kjørlaug et al. (2014). The maximum equivalent stress induced by El Centro earthquake at the bottom of the structure considering SSI was higher than the yield stress (Figures 11.(c,e)). In the non-linear analysis, a plastic deformation took place in the structure according to the bilinear kinematic hardening material model (Figure 11.(e)). The value of the stresses were slightly lower due the consideration of the non-linear stress/strain relationship.

Figure 12 presents the equivalent stresses at the time steps where the maximum values were reached. The deformed shape practically corresponded with the second bending mode shape and, therefore, the maximum stress in the tower was located about the half of its length. The time where the maximum stress occurred is different for each analysis because of the different natural period of the structure when SSI is considered or not.

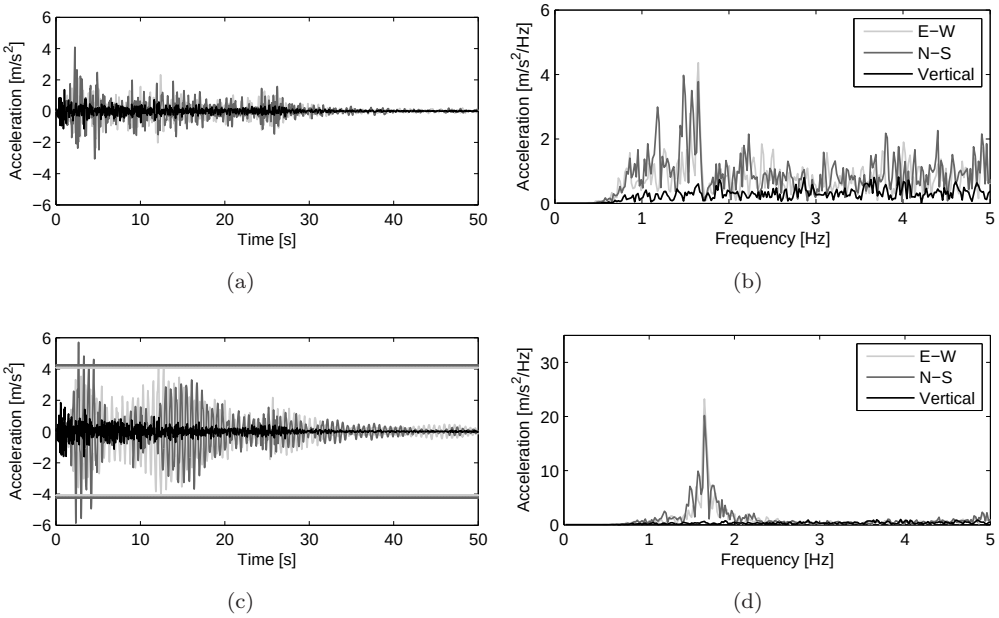

Figure 10.: (a,c) Time history and (b,d) frequency content of acceleration at longitudinal, transversal and vertical directions at (a,b) the bottom and (c,d) the top of the wind turbine induced by El Centro (1940) accelerogram for turbine 2 considering the soil type F. In Figure 10.(c) the horizontal lines indicate the maximum acceleration computed from a seismic response spectrum analysis without SSI at the top of the wind turbine.

5. Conclusions

The response of wind turbines is induced by wind, transient and cyclic loads from operational procedures, and extreme loads such as earthquakes. An accurate evaluation of the natural frequencies of the system is needed for the structural design to avoid the excitation of resonance frequencies in operational conditions. From the literature, it can be concluded that the effect of SSI is important, and it should not be neglected. In this paper, the dynamic behaviour of wind turbines considering different soil conditions using a general purpose three dimensional BEM-FEM model formulated in time domain has been studied.

Firstly, the design approach of three wind turbines was obtained by comparison of their natural frequencies without SSI and the rotor speed. Soft-soft, soft-stiff, stiff-stiff designs were considered. Then, the natural frequencies and damping of the structures were computed with the proposed methodology, considering the monopile foundation and the surrounding soil. The foundation-soil interaction increased the overall structural damping and reduced the natural frequencies. The obtained results show that, if the design type is determined according to simplified expressions that neglect the SSI for evaluating the natural frequencies, then the determination of the design type might be wrong. Thus, SSI should be considered for ensuring a proper and safe design-type classification.

As a case study, the response of the structures due to extreme loads was also analysed. The proposed model allowed to study the seismic response of the wind turbine due to an incident SH wave and El Centro earthquake. The response of the wind turbines was characterised from the natural frequencies and the frequency content of the incident wave-field. Therefore, it is necessary to compute accurately the modal parameters of the structures.

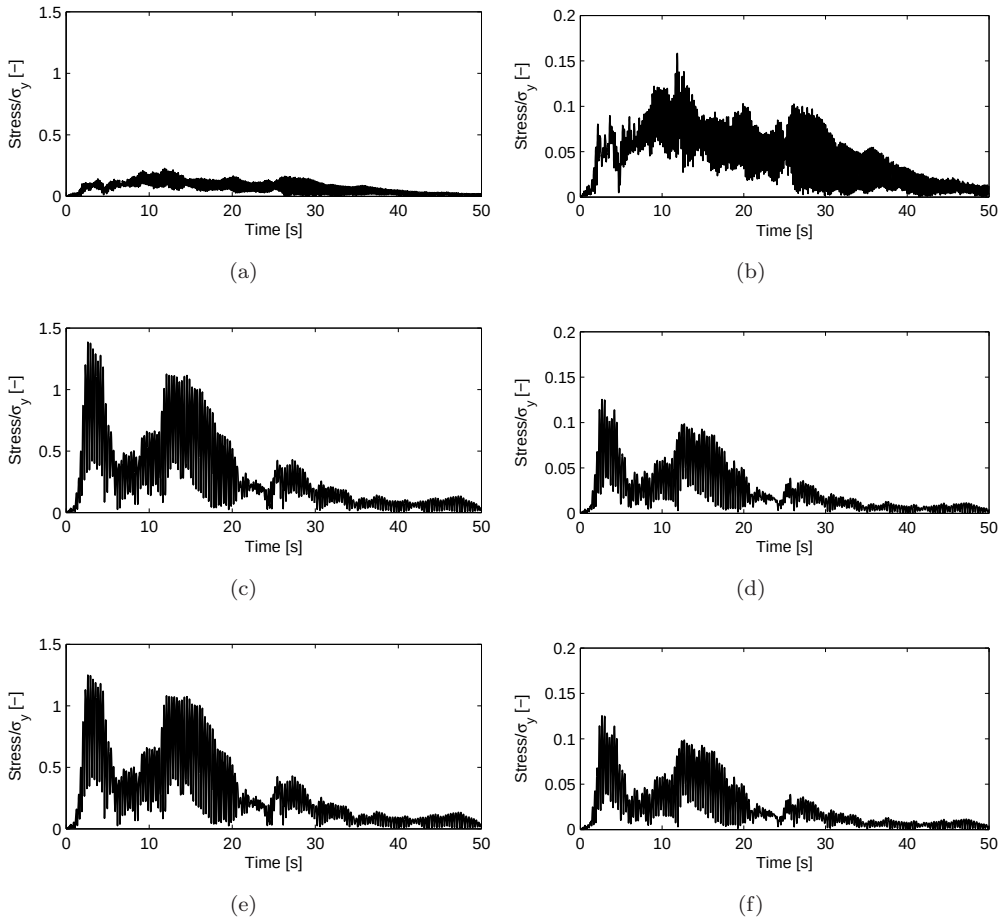

Figure 11.: Time histories of normalized stresses at (a,c,e) the top of the foundation and (b,d,f) at the half length of the wind turbine 2 induced by El Centro (1940) earthquake (a,b) without soil-structure interaction and linear analysis, and considering the soil type F and (c,d) linear analysis and (e,f) non-linear analysis.

Acknowledgments

The authors would like to thank to the reviewers for their valuable comments, ideas and suggestions that have certainly permitted to raise the manuscript quality.

This research was funded by the Spanish Ministry of Economy and Competitiveness (Ministerio de Economía y Competitividad) through research project BIA2013-43085-P and the Consejería de Economía, Innovación, Ciencia y Empleo of Andalucía under project P12-TEP-2546. Financial support is gratefully acknowledged.

References

Adhikari S., Bhattacharya, S. (2011). Vibrations of wind-turbines considering soil-structure interaction. Wind and Structures. 14, 85–112.

Adhikari S., Bhattacharya, S. (2012). Dynamic analysis of wind turbine towers on flexible foundations on flexible foundations. Shock and Vibration. 19, 37–56.

Andersen, L.V., Vahdatirad, M.J., Sichani, M.T, Sørensen, J.D. (2012). Natural frequencies of wind turbines on monopile foundations in clayey soils-A probabilistic approach. Computers and Geotechnics. 43, 1–11.

American Society of Civil Engineers (2010). Minimum Design Loads for Buildings and Other Structures. ASCE/SEI 7-10. Technical standard.

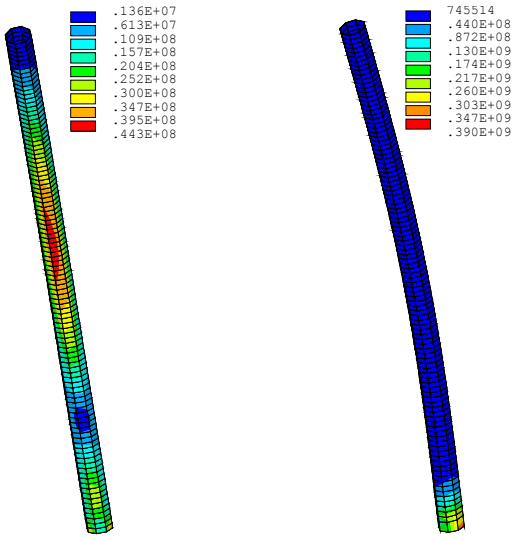

(a) (b)

Figure 12.: Equivalent stresses at turbine 2 induced by El Centro (1940) earthquake (a) at time $t = 11.86\,\mathrm{s}$ without soil-structure interaction, and (b) at time $t = 2.97\,\mathrm{s}$ considering the soil type F.

Bhattacharya, S., Adhikari S. (2011). Experimental validation of soil-structure interaction of offshore wind turbines. Soil Dynamics and Earthquakes Engineering. 31, 805–816.

Bhattacharya, S., Nikitas, N., Garnsey, J., Alexander, N.A., Cox, J., Lombardi, D., Muir Wood, D., Nash, D.F.T (2013). Observed dynamic soil-structure interaction in scale testing of offshore wind turbine foundations. Soil Dynamics and Earthquakes Engineering. 54, 47–60.

Bisoi, S., Haldar, S. (2014). Dynamic analysis of offshore wind turbine in clay considering soil-monopile-tower interaction. Soil Dynamics and Earthquakes Engineering. 63, 19–35.

Bisoi, S., Haldar, S. (2015). Design of monopile supported offshore wind turbine in clay considering dynamic soil-structure-interaction. Soil Dynamics and Earthquakes Engineering. 73, 103–117.

Borcherdt, R. D., (1994). Estimates of site-dependent response spectra for design (Methodology and Justification). Earthquake Spectra. 10, 617–653.

Clough, R.W., Penzien, J. (1975). Dynamic of Structures, McGraw-Hill, New York.

Clouteau, D., Cottereau, R., Lombaert, G. (2013). Dynamics of structures coupled with elastic media - A review of numerical models and methods. Journal of Sound and Vibration. 332, 2415–2436.

Damgaard, M., Ibsen, L.B., Andersen, L.V., Andersen, J.K.F. (2013). Cross-wind modal properties of offshore wind turbines identified by full scale testing. Journal of Wind Engineering and Industrial Aerodynamics. 116, 94–108.

Damgaard, M., Zania, V., Andersen, L.V., Ibsen, L.B. (2014). Effects of soil-structure interaction on real time dynamic response of offshore wind turbines on monopiles. Engineering Structures. 75, 388–401.

Domínguez, J. (1993). Boundary elements in dynamics, Computational Mechanics Publications and Elsevier Applied Science, Southampton.

Eringen, A.C., Suhubi, E.S. (1975). Elastodynamics, Volume 2, Linear theory. Academic Press, New York, USA.

European Wind Energy Association (2014). Wind energy scenarios for 2020. Technical report.

Fischer, T. (2006). Offshore foundation and support structures. Technical report.

Galvín, P., Domínguez J. (2007). Analysis of ground motion due to moving surface loads induced by high-speed trains. Engineering Analysis with Boundary Elements. 31, 931–941.

Galvín, P., Romero, A., Domínguez, J. (2010). Fully three-dimensional analysis of high-speed train-track-soil-structure dynamic interaction. Journal of Sound and Vibration. 329, 5147–5163.

Galvín, P., Romero, A. (2014). A MATLAB toolbox for soil-structure interaction analysis with finite and boundary elements. Soil Dynamics and Earthquake Engineering. 57, 10–14.

Harte, M., Basu, B., Nielsen, S.R.K. (2012). Dynamic analysis of wind turbines including soil-structure interaction. Engineering Structures. 45, 509–518.

Hermanns, L., Santoyo, M.A., Quirós, L.E., Vega, J., Gaspar-Escribano, J.M., Benito B. (2011). Dynamic response of wind turbines to theoretical 3D seismic motions taking into account the rotational component. International Science Index 59, 944–947.

International Electrotechnical Commission (2005). IEC 61400-1. Wind turbines - part 1: design requirements. Technical standard.

Kaynia, A.M., Kausel, E. (1991). Dynamics of piles and pile groups in layered soil media. Soil Dynamics and Earthquake Engineering. 10, 386–401.

Kausel, E. (2010). Early history of soil-structure interaction. Soil Dynamics and Earthquake Engineering. 30, 822–832.

Kjørlaug R.A., Kaynia A.M., Elgamal, A. (2014). Seismic Response of Wind Turbines due to Earthquake and Wind Loading. Proceedings of the 9th International Conference on Structural Dynamics, EURODYN 2014. Porto, Portugal, Cunha A., Caetano E., Ribeiro P., Müller G. (eds.).

Kühn, M. (2003). Dynamics and design optimisation of offshore wind energy conversion systems. PhD thesis, Delft University.

Lombardi, D., Bhattacharya, S., Wood, D.M. (2013). Dynamic soil-structure interaction of monopile supported wind turbines in cohesive soil. Soil Dynamics and Earthquakes Engineering. 49, 165–180.

Manwell, J.F., McGowan, J.G., Rogers, A.L. (2002). Wind Energy Explained - Theory, Design and Application, John Wiley & Sons Lt.

Magalhaẽs, F., Cunha, A., Caetano, E., Brincker, R. (2010). Damping estimation using free decays andambient vibration tests. Mechanical Systems and Signal Processing. 24, 1274–1290.

Negro, V., López-Gutiérrez, J.S., Esteban, M.D., Matutano, C. (2014). Uncertainties in the design of support structures and foundations for offshore wind turbines. Renewable Energy. 63, 125–132.

Newmark N.M. (1959). A method of computation for structural dynamics. ASCE Journal of the Engineering Mechanics Division. 85, 67–94.

Papagiannopoulos, G.A., Beskos, D.E. (2006). On a modal damping identification model of building structures. Archive of Applied Mechanics. 76, 443–63.

Prabucki, M.J., Estorff, O. von (1990). Dynamic response in the time domain by coupled boundary and finite elements. Computational Mechanics. 6, 35–46.

Romero, A., Galvín, P., Domínguez, J. (2013). 3D non-linear time domain FEM-BEM approach to soil-structure interaction problems. Engineering Analysis with Boundary Elements. 37, 501–512.

Sapountzakis E.J., Dikaros I.C., Kampitsis A.E., Koroneou A.D. (2015). Nonlinear response of wind turbines under wind and seismic excitations with soil-structure interaction. Journal of Computational Nonlinear Dynamics. 10, 041007-041007–16.

Shirzadeh, R., Devriendt, C., Bidakhvidi, M.A., Guillaume, P. (2013). Experimental and computational damping estimation of an offshore wind turbine on a monopile foundation. Journal of Wind Engineering and Industrial Aerodynamics. 120, 96–106.

Tempel, D.P., Molenaar, D.P. (2002). Wind turbine structural dynamics - a review of the principles for modern power generation, onshore and offshore. Wind Engineering. 26, 211-220.

Van der Woude, C., Narasimhan, S. (2014). A study on vibration isolation for wind turbine structures. Engineering Structures. 60, 223–234.

Wolf, J.P. (1985). Dynamic soil-structure interaction. Prentice-Hall, Englewood Cliffs, N.J.

Zania, V. (2013). Natural vibration frequency and damping of slender structures founded on monopiles. Soil Dynamics and Earthquakes Engineering. 59, 8–20.

Zienkiewicz, O.C. (1986). The finite element method. McGraw-Hill.